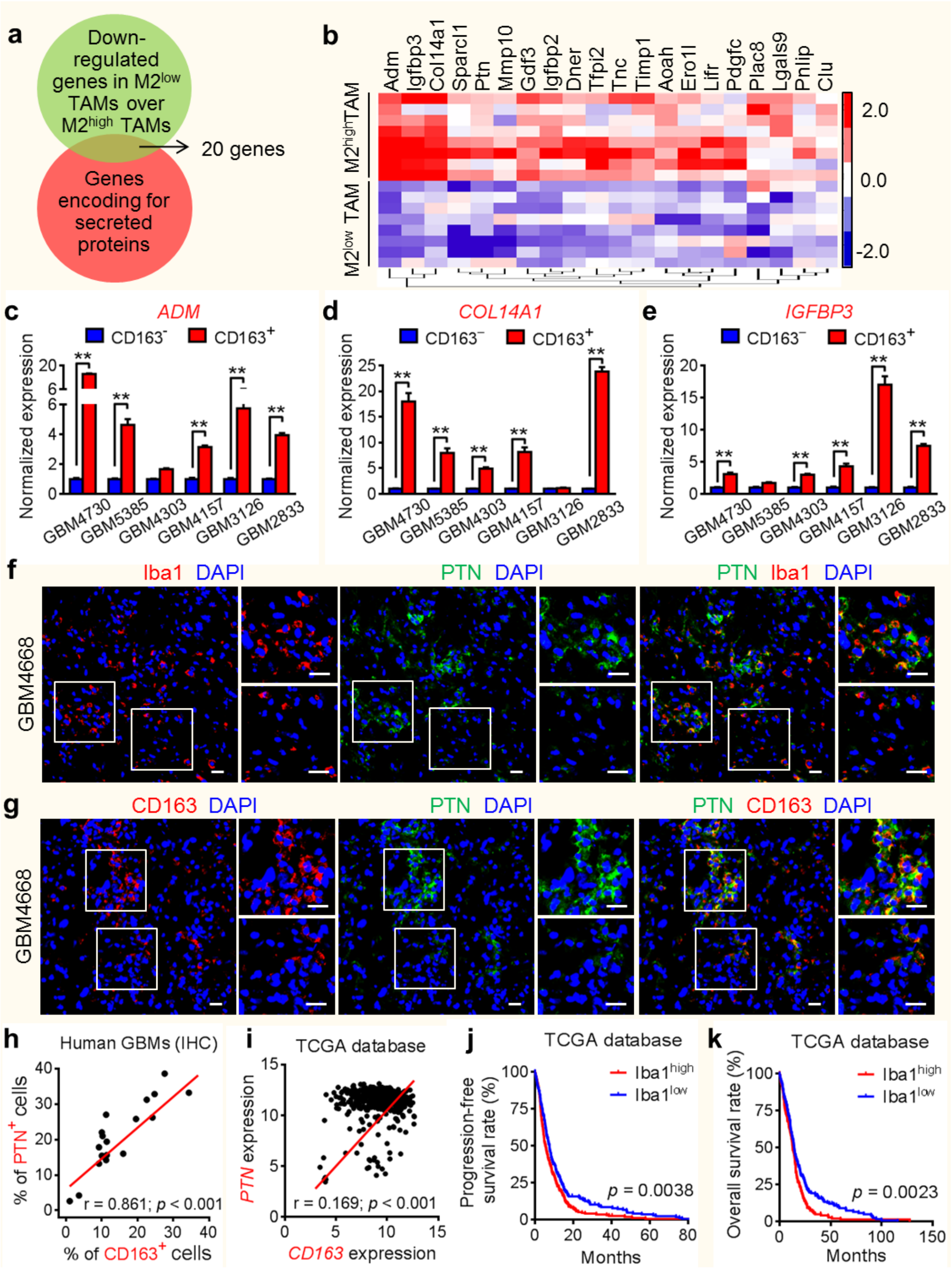

Supplementary Figure 1. PTN is co-enriched with CD163$^+$ M2 TAMs in human GBMs.

(**a**) Venn diagram showing gene candidates with reduced expressions in M2^{low} TAMs (GEO, GSE37475) and overlapped with those encoding for secreted proteins (Secreted Protein Database, http://spd.cbi.pku.edu.cn/). M2^{low} TAMs were induced by the treatment of CSF-1 receptor inhibitor BLZ945 to suppress M2 polarization and were isolated from murine gliomas.

(**b**) Heatmap of the secreted protein-coding genes with reduced expression in M2^{low}

TAMs relative to M2^{high} TAMs identified from (**a**).

(**c-e**) qRT-PCR analyses of the expression of *ADM* (**c**), *COL14A1* (**d**), or *IGFBP3* (**e**) between FACS-sorted CD11b$^+$/CD163$^+$ M2 TAMs and CD11b$^+$/CD163$^-$ control TAMs from 6 cases of human GBMs. Data are shown as means ± s.e.m., $^{**}p < 0.01$, student's *t*-test.

(**f-g**) Immunofluorescent staining of PTN (in green) and the TAM marker Iba1 (in red, **f**) or the M2 TAM marker CD163 (in red, **g**) in human GBMs. Scale bar represents 25 μm.

(**h-i**) Bivariate correlation analyses of the expressions of PTN and M2 TAM marker CD163 in human GBMs as examined by IHC staining (**h**) or by bioinformatic analyses of the gene profiling data from the TCGA database (**i**). $p < 0.001$, Pearson *r* test.

(**j-k**) Kaplan-Meier survival analysis of Iba1 expression and the progression-free survival (**j**) or overall survival (**k**) of GBM patients from the TCGA database. The cut-off point for stratification was generated using X-tile software according to Iba1 level. $p = 0.0038$ (**j**), $p = 0.0023$ (**k**), log-rank test.

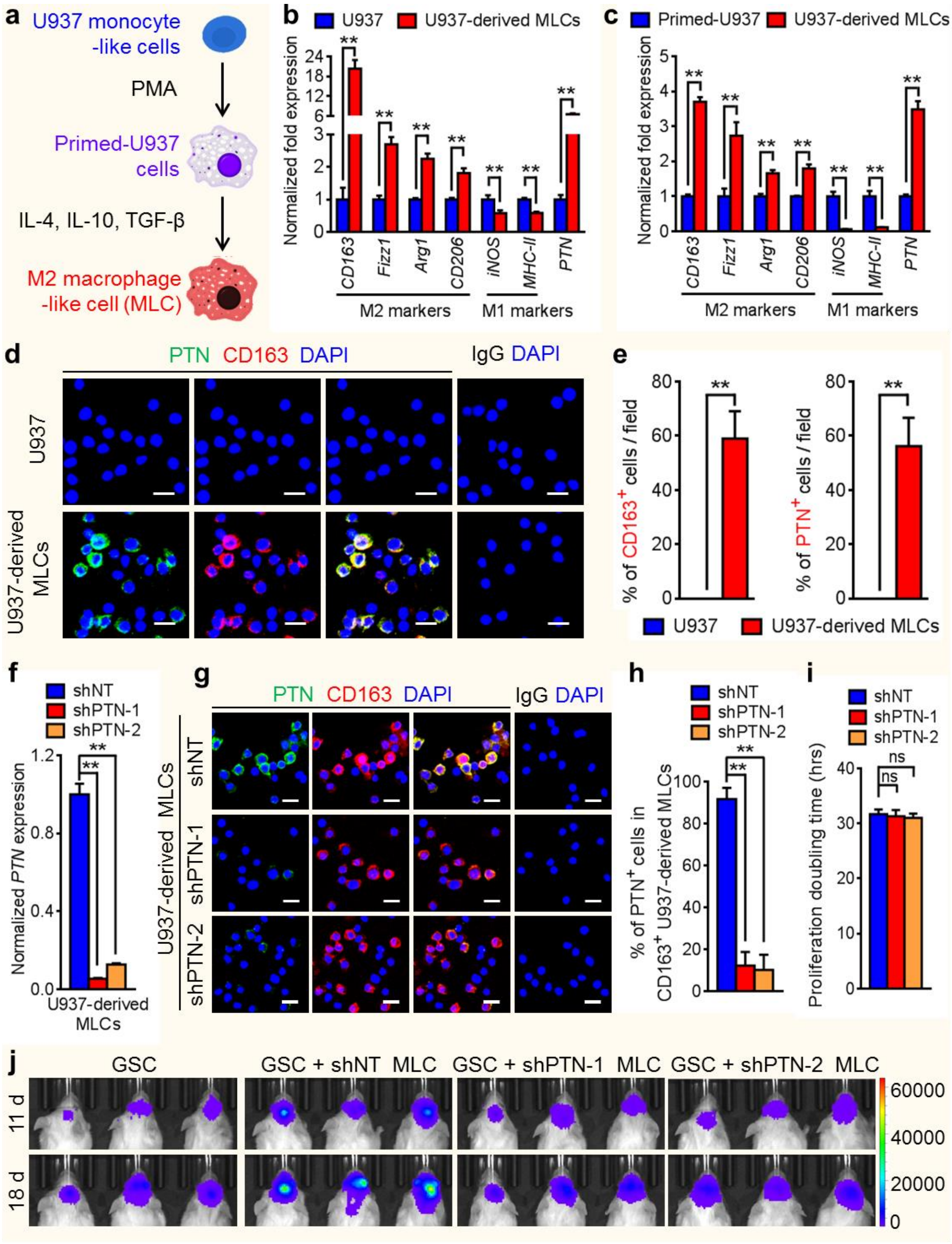

Supplementary Figure 2. U937-derived MLCs harbor M2 TAM properties and recapitulate the tumour-supportive functions of M2 TAMs *in vivo*.

(**a**) A schematic diagram showing the polarization of U937 monocytes into M2 macrophage-like cells (MLCs).

(**b-c**) qRT-PCR analyses of the expressions of M2 markers (*CD163*, *Fizz1*, *Arg1* and *CD206*), M1 markers (*iNOS* and *MHC-II*) and *PTN* between U937 and the U937-derived MLCs (**b**) or between primed-U937 and the U937-derived MLCs (**c**). Data are shown as means ± s.e.m., $^{**}p < 0.01$, student's *t*-test.

(**d-e**) Immunofluorescent staining (**d**) of PTN (in green) and the M2 TAM marker CD163 (in red) in U937 and the U937-derived MLCs. The quantification of $CD163^+$ cells (**e**, left panel) or PTN^+ cells (**e**, right panel) is shown. Scale bar represents 20 μm. Data are shown as means ± s.d., ***p* < 0.01, student's *t*-test.

(**f-h**) qRT-PCR analysis (**f**) and immunofluorescent staining (**g, h**) of PTN expression in the MLCs expressing shPTN or shNT control. Scale bar represents 20 μm. Data are shown as means ± s.d., ***p* < 0.01, ANOVA test.

(**i**) The doubling time of the U937-derived MLCs expressing shPTN or shNT control. Data are shown as means ± s.d., ns, not significant, ANOVA test. Hrs, hours.

(**j**) The bioluminescent images of intracranial GBM xenografts implanted with GSCs only or co-implanted with GSCs and MLCs expressing shPTN or shNT at the indicated time points.

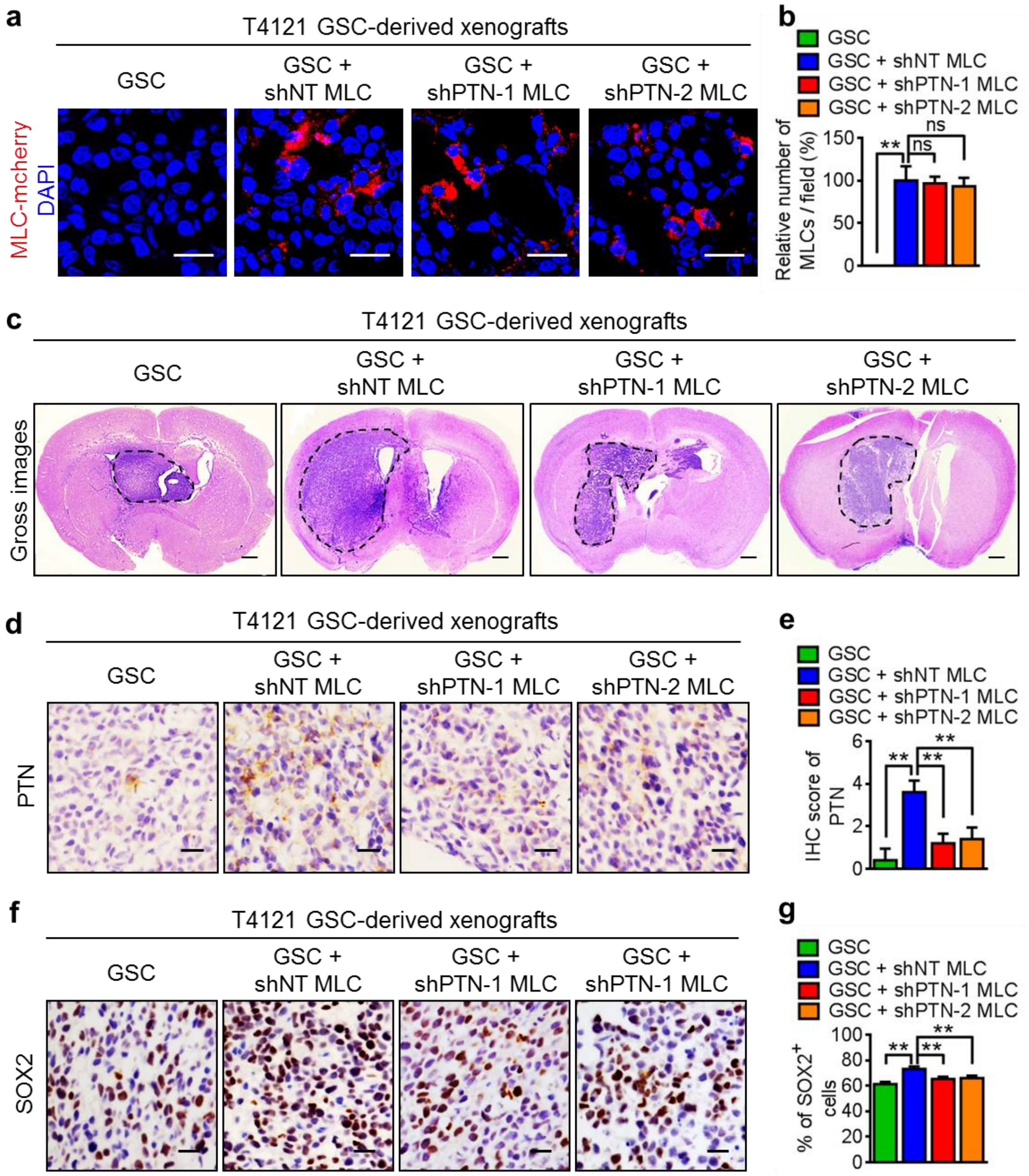

Supplementary Figure 3. U937-derived MLCs promote GSC tumour growth and increase the level of PTN in GSC xenografts.

(**a-b**) Representative immunofluorescent images of mCherry-labelled MLCs (**a**, in red) and the relative number of mCherry^+ MLCs (**b**) in GBM xenografts implanted with GSCs only or co-implanted with GSCs and MLCs expressing shPTN or shNT. The number of mCherry^+ MLCs of each group relative to the GSC + shNT MLC group was presented. Scale bar represents 25 μm. Data are shown as means ± s.d., $^{**}p < 0.01$, ns, not significant, ANOVA test.

(**c**) Hematoxylin and eosin (H&E) staining of the cross sections of mouse brains bearing xenografts derived from GSC, GSC + shNT MLC or GSC + shPTNs MLC. The dashed line indicated the xenograft regions in mouse brain. Scale bar represents 500 μm.

(**d-e**) Representative IHC images (**d**) and the quantification (**e**) of PTN in GBM xenografts derived from GSC, GSC + shNT MLC or GSC + shPTNs MLC. Scale bar represents 25 μm. Data are shown as means ± s.d., $^{**}p < 0.01$, ANOVA test.

(**f-g**) Representative IHC images of SOX2 (**f**) and the percentage of GSCs marked by SOX2 (**g**) in xenografts derived from GSC, GSC + shNT MLC or GSC + shPTNs MLC. Scale bar represents 25 μm. Data are shown as means ± s.d., $^{**}p < 0.01$, ANOVA test.

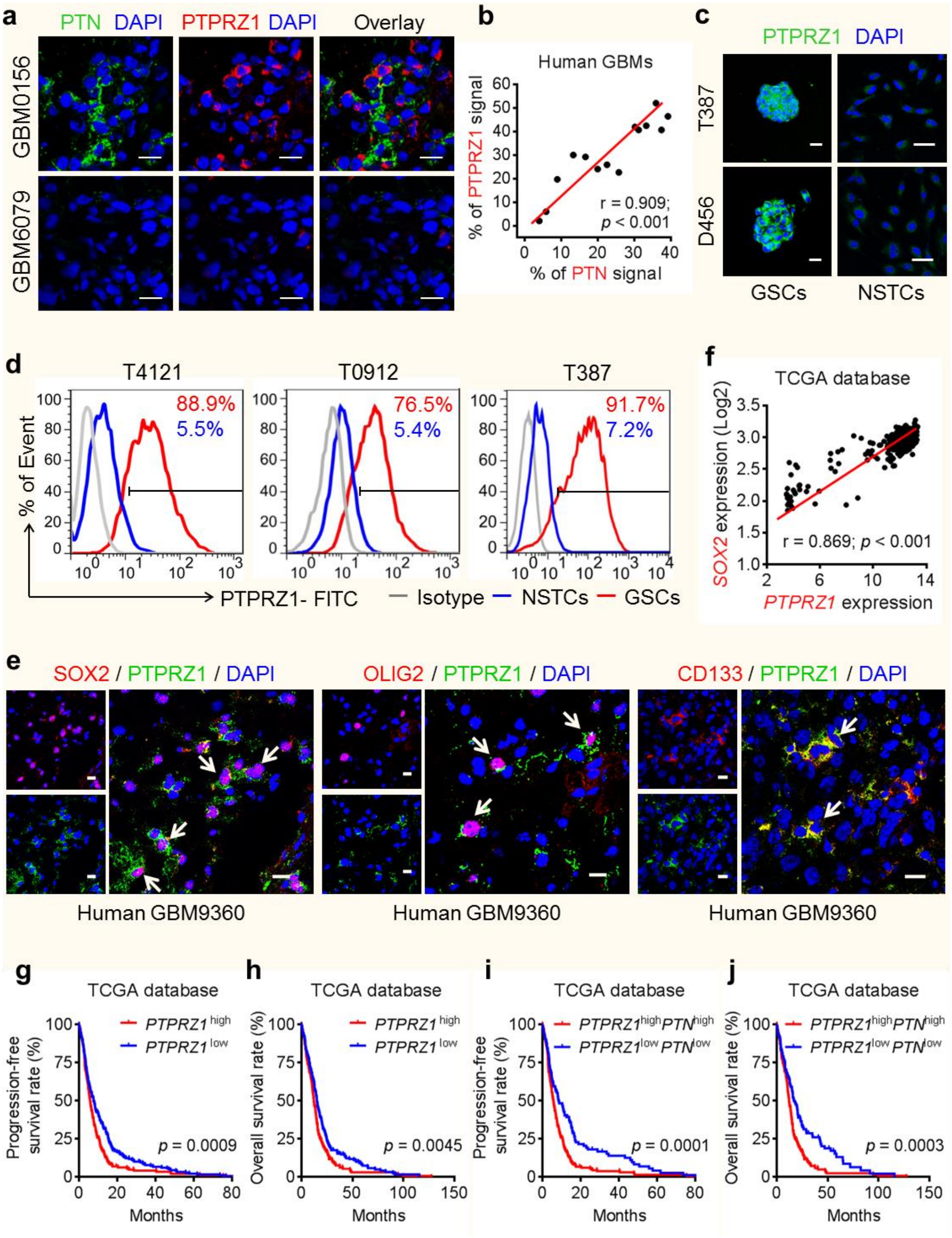

Supplementary Figure 4. PTPRZ1 is preferentially expressed in GSCs and combines with PTN to predict poor prognosis of patients with GBM.

(**a**) Representative immunofluorescent stainings of PTN (in green) and PTPRZ1 (in red) in human GBMs. Scale bar represents 20 μm.

(**b**) Bivariate correlation analyses showing a positive correlation of PTN and PTPRZ1 expressions as examined by immunofluorescent stainings shown in (**a**) in human GBMs. $p < 0.001$, Pearson r test.

(**c**) Immunofluorescence of PTPRZ1 (in green) in GSC tumourspheres and NSTCs isolated from T387 and D456 human GBM xenografts. Scale bar represents 25 μm.

(**d**) Flow cytometry analysis of PTPRZ1 expression in GSCs and matched NSTCs from T4121, T0912 and T387 GBMs.

(**e**) Co-immunofluorescent stainings of PTPRZ1 (in green) and the GSC marker SOX2 (in red, left panel), OLIG2 (in red, middle panel) or CD133 (in red, right panel) in human GBMs. Scale bar represents 25 μm.

(**f**) Bivariate correlation analyses showing a positive correlation of PTPRZ1 and the GSC marker SOX2 in 541 cases of human GBMs from the TCGA database. $p < 0.001$, Pearson *r* test.

(**g**, **h**) Kaplan-Meier survival analysis of PTPRZ1 expression and the progression-free survival (**g**) or overall survival (**h**) of patients with GBM from the TCGA database. The cut-off point for stratification was generated using X-tile software according to the PTPRZ1 level. Log-rank test.

(**i**, **j**) Kaplan-Meier survival analyses of the combined PTPRZ1 and PTN expressions and the progression-free survival (**i**) or overall survival (**j**) of patients with GBM from the TCGA database. The cut-off point for stratification was generated using X-tile software according to the PTPRZ1 and PTN levels. Log-rank test.

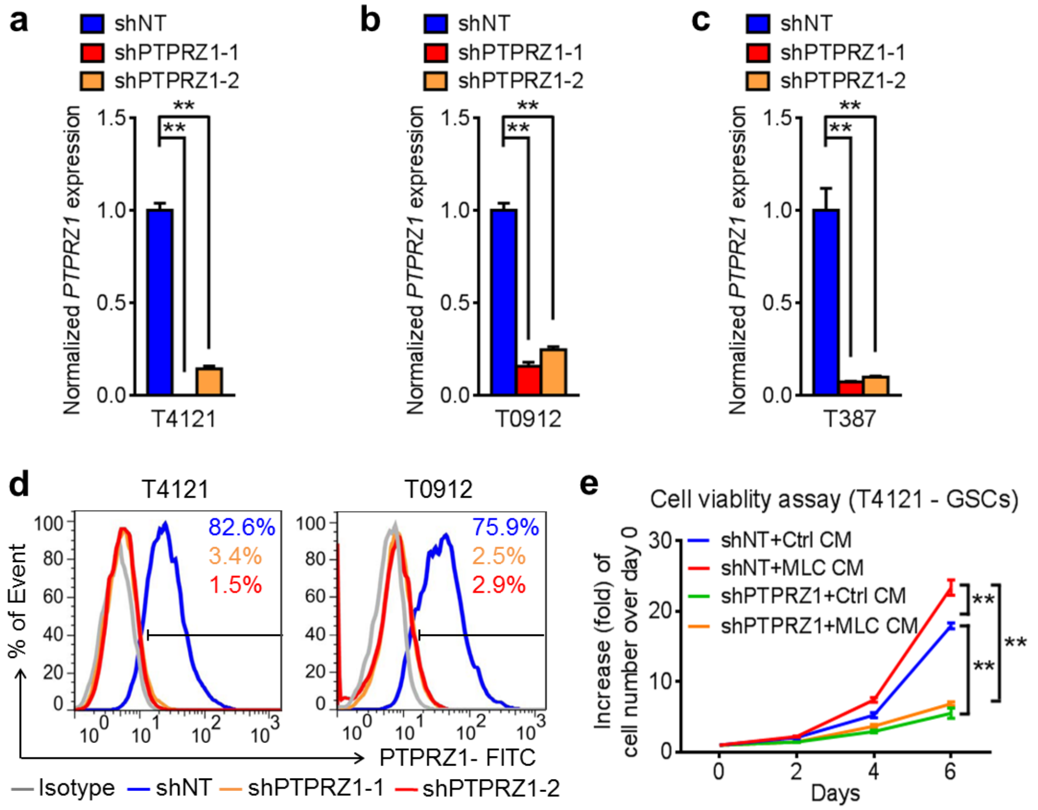

Supplementary Figure 5. ShRNAs against PTPRZ1 reduce PTPRZ1 expression in GSCs and compromise the tumour-supportive role of TAMs on GSC proliferation

(**a-c**) qRT-PCR analyses showing the level of *PTPRZ1* in GSCs expressing shPTPRZ1 was significantly lower than the GSCs expressing the shNT control. GSCs were derived from T4121 (**a**), T0912 (**b**) or T387 (**c**) human GBM xenografts. Data are shown as means ±s.e.m., **p < 0.01, ANOVA test.

(**d**) Flow cytometry analysis of PTPRZ1 expression in T4121 and T0912 GSCs expressing shPTPRZ1 or the shNT control.

(**e**) Cell viability assay of GSCs cultured in the conditioned medium of MLCs. Data are shown as means ±s.d., **p < 0.01, ANOVA test.

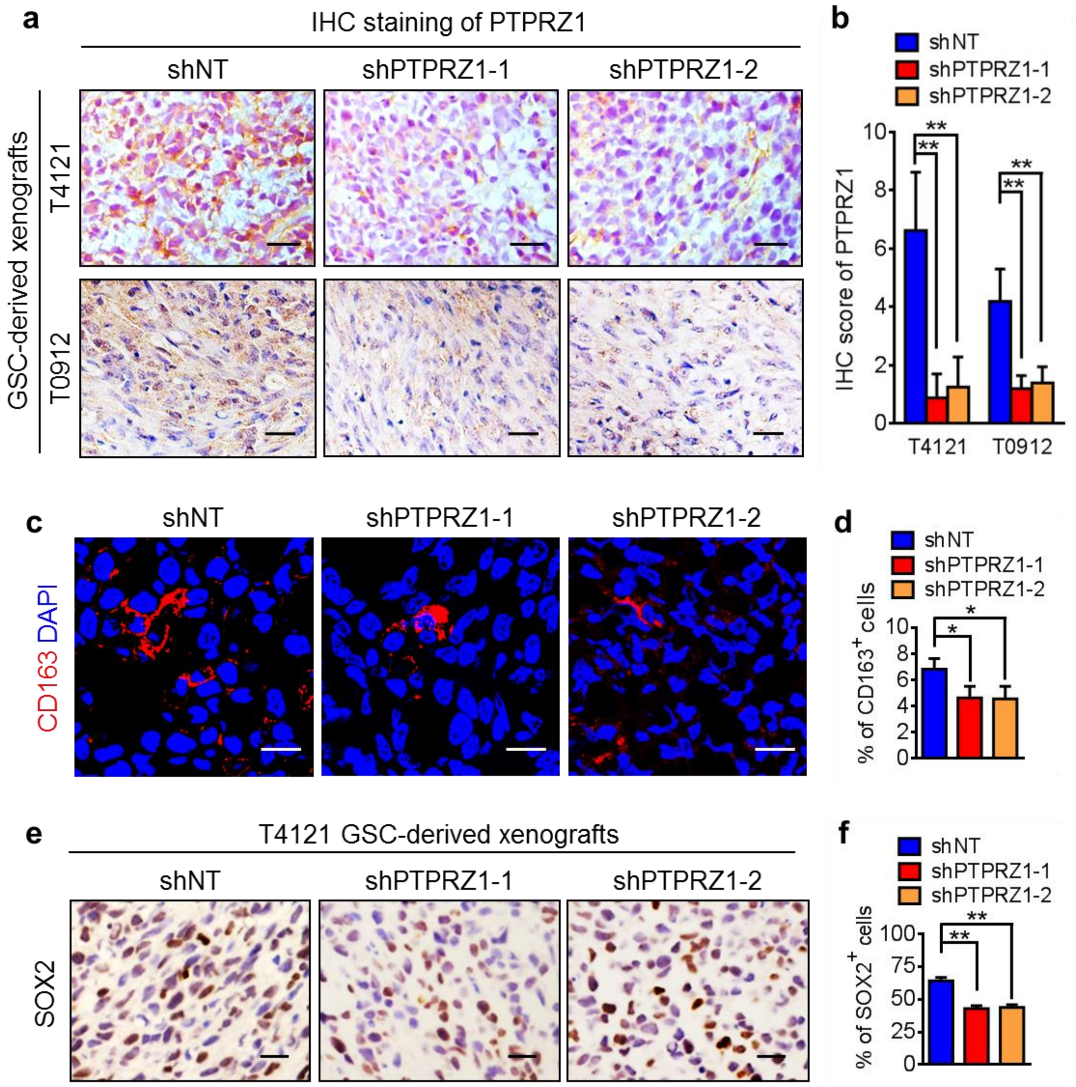

Supplementary Figure 6. Disrupting PTPRZ1 expression in GSCs impairs TAM infiltration, reduces GSC proportion in GSC xenografts.

(**a, b**) Representative IHC images (**a**) and the quantification (**b**) of PTPRZ1 expression in xenografts derived from T4121 GSCs (upper panels) or T0912 GSCs (lower panels) expressing shPTPRZ1 or shNT control. PTPRZ1 expression was scored according to the proportion of positive tumour cells and the staining intensity. Data are shown as means ±s.d., **p < 0.01, ANOVA test. Scale bar represents 25 μm.

(**c, d**) Representative immunofluorescent images (**c**) and the percentage (**d**) of infiltrating TAMs marked by CD163 in xenografts derived from T4121 GSCs expressing shPTPRZ1 or shNT. Data are shown as means ± s.d., *$p < 0.05$, ANOVA test. Scale bar represents 25 μm.

(**e, f**) Representative IHC images of SOX2 (**e**) and the percentage of GSCs marked by SOX2 (**f**) in xenografts derived from T4121 GSCs expressing shPTPRZ1 or shNT. Data are shown as means ± s.d., **$p < 0.01$, ANOVA test. Scale bar represents 25 μm.

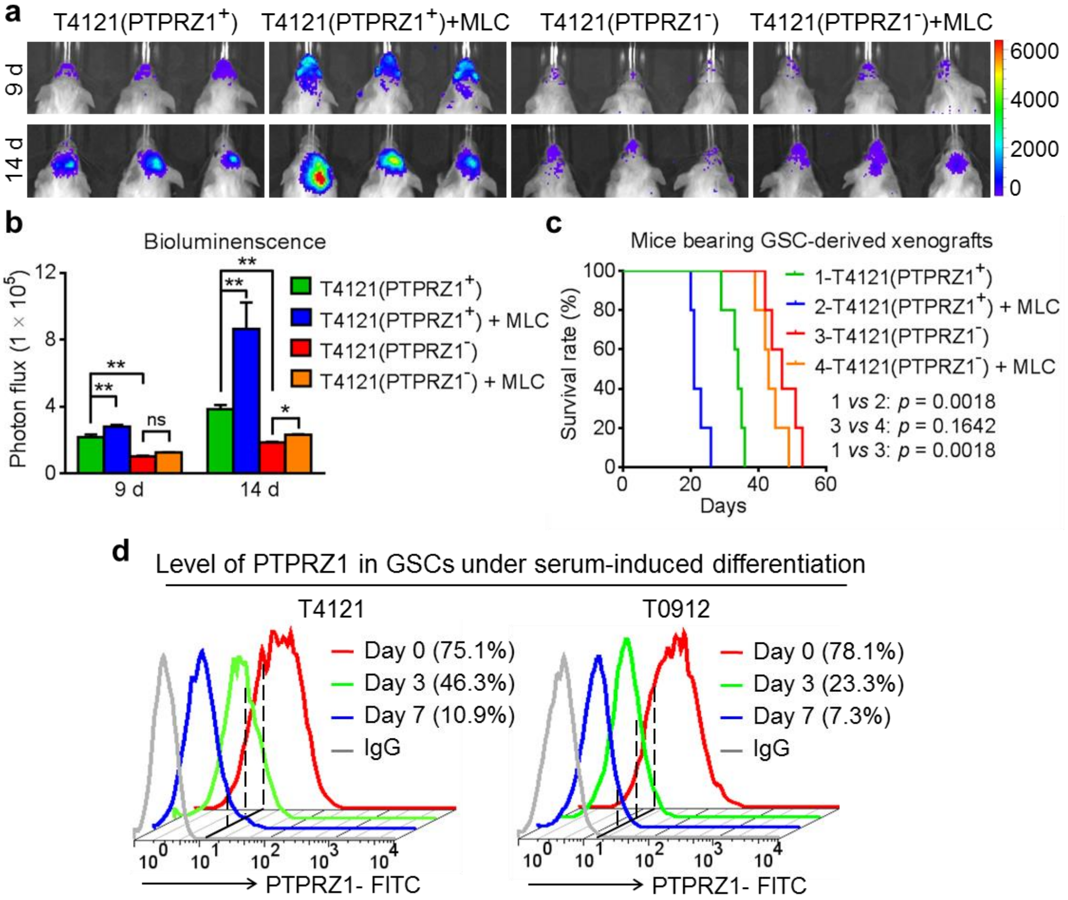

Supplementary Figure 7. TAMs promote the tumour growth of PTPRZ1^{+} glioma cells that are enriched with GSCs.

(**a-b**) Representative bioluminescent images (**a**) and the quantification (**b**) of the intracranial xenografts derived from PTPRZ1^{+} glioma cells, PTPRZ1^{+} glioma cells + MLCs, PTPRZ1^{-} glioma cells or PTPRZ1^{-} glioma cells + MLCs. Data are shown as means ± s.e.m., **$p < 0.01$, *$p < 0.05$, ns, not significant, ANOVA test.

(**c**) Kaplan-Meier analyses of mice bearing PTPRZ1^{+} glioma cells, PTPRZ1^{+} glioma cells + MLCs, PTPRZ1^{-} glioma cells or PTPRZ1^{-} glioma cells + MLCs. Log-rank test.

(**d**) Flow cytometry analysis of PTPRZ1 expression in GSCs (T4121 and T0912) cultured in serum-induced differentiation medium over a 7-day period.

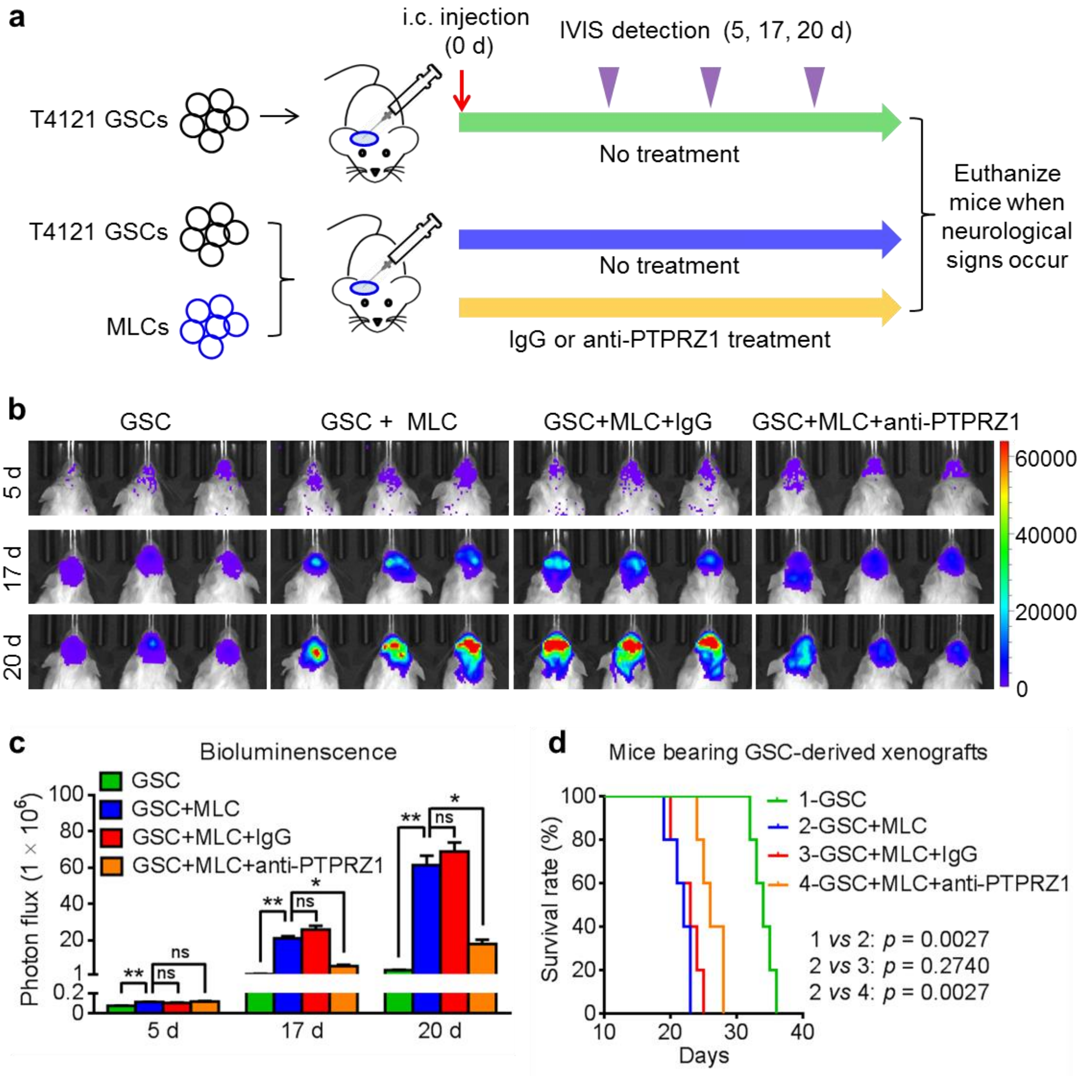

Supplementary Figure 8. Anti-PTPRZ1 treatment inhibits GSC tumour growth and prolongs animal survival.

(**a**) Schematic diagram of GSC-driven xenografts co-implanted with MLCs in combination with the treatment of anti-PTPRZ1 antibody. After implantation, mice were left untreated (GSC control or GSC+MLC control) or treated with the anti-PTPRZ1 antibody or isotype IgG every two days until moribund. Tumour growth was monitored through the IVIS bioluminescent imaging system and mice were euthanized when neurological signs occurred.

(**b, c**) Representative bioluminescent images (**b**) and the quantification (**c**) of intracranial GBM xenografts derived from GSC or GSC+MLC treated with anti-PTPRZ1 antibody or isotype IgG control at the indicated time points after cell transplantation. GSCs were transduced with luciferase-expressing vector before implantation. n = 5 per group. Data are shown as means ± s.e.m., $*p < 0.05$, $**p < 0.01$, ns, not significant, ANOVA test.

(**d**) Kaplan-Meier survival analysis of mice implanted with GSC or GSC+MLC in combination with the treatment of anti-PTPRZ1 antibody. n = 5, log-rank test.

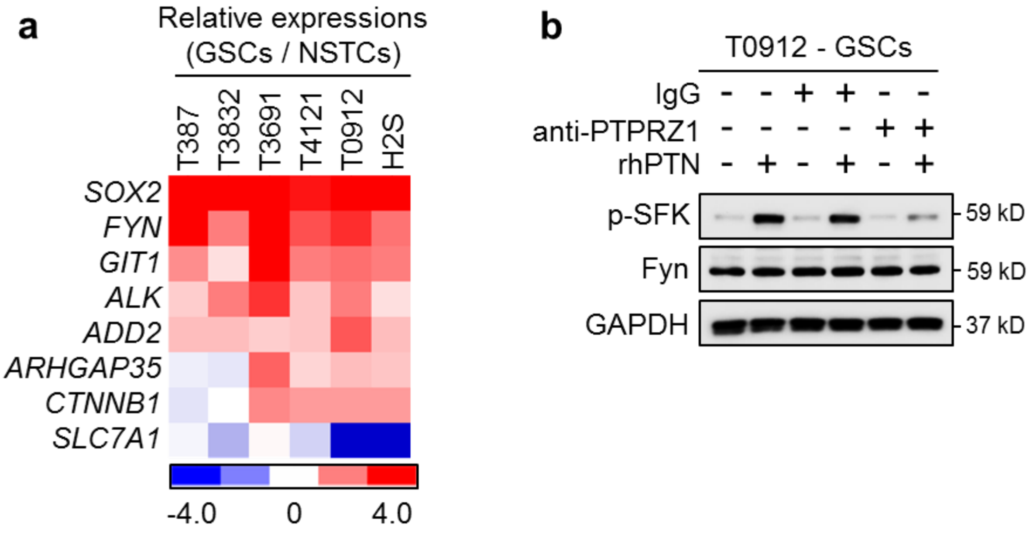

Supplementary Figure 9. The PTN-PTPRZ1 signaling regulates Fyn kinase phosphorylation.

(**a**) qRT-PCR analyses of the expressions of seven identified downstream targets of PTPRZ1 in 6 pairs of GSCs and matched NSTCs isolated from primary GBMs. The GSC marker *SOX2* was employed as the positive control. The data were presented as heatmap using Cluster/Java Treeview.

(**b**) Immunoblot analyses of phospho-Src family kinase (p-SFK, Tyr416) and Fyn in T0912 GSCs, showing that rhPTN stimulation markedly increased activating phosphorylation of SFK (p-Tyr416), while the anti-PTPRZ1 antibody treatment largely abrogated SFK activation in GSCs.

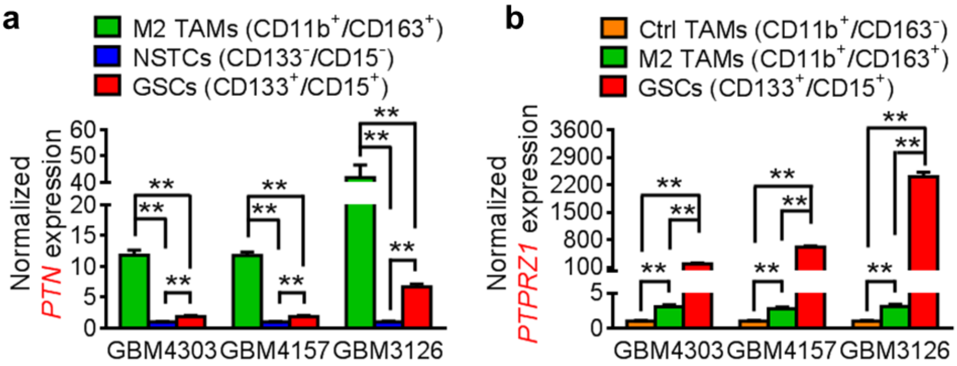

Supplementary Figure 10. PTN is preferentially expressed in CD163$^+$ M2 TAMs and PTPRZ1 is preferentially expressed in GSCs in human GBMs.

(**a**) qRT-PCR analyses of *PTN* expression in M2 TAMs (CD11b$^+$/CD163$^+$), NSTCs (CD133$^-$/CD15$^-$) and GSCs (CD133$^+$/CD15$^+$) from 3 cases of human GBMs. Data are shown as means ± s.e.m., $^{**}p < 0.01$, ANOVA test.

(**b**) qRT-PCR analyses of *PTPRZ1* expression in M2 TAMs (CD11b$^+$/CD163$^+$), control TAMs (CD11b$^+$/CD163$^-$) and GSCs (CD133$^+$/CD15$^+$) from 3 cases of human GBMs. Data are shown as means ± s.e.m., $**p < 0.01$, ANOVA test.

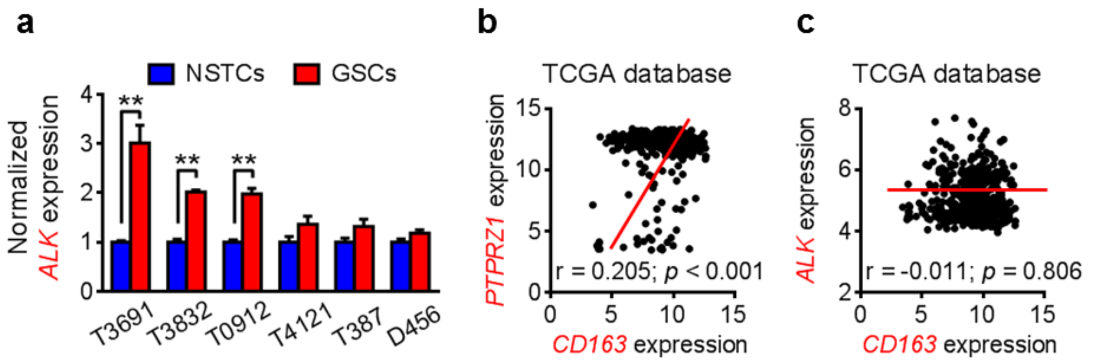

Supplementary Figure 11. PTPRZ1 rather than ALK is more likely to be associated with GSC phenotypes and mediates the crosstalk between GSCs and TAMs.

(**a**) qRT-PCR analysis of *ALK* in GSCs and matched NSTCs derived from human GBMs. Data are shown as means ± s.e.m., $**p < 0.01$, student's *t*-test.

(**b-c**) Bivariate correlation analyses of *CD163* and *PTPRZ1* (**b**) or *ALK* (**c**) in human GBMs from the TCGA database. $p < 0.001$ (**b**), $p = 0.806$ (**c**), Pearson *r* test.

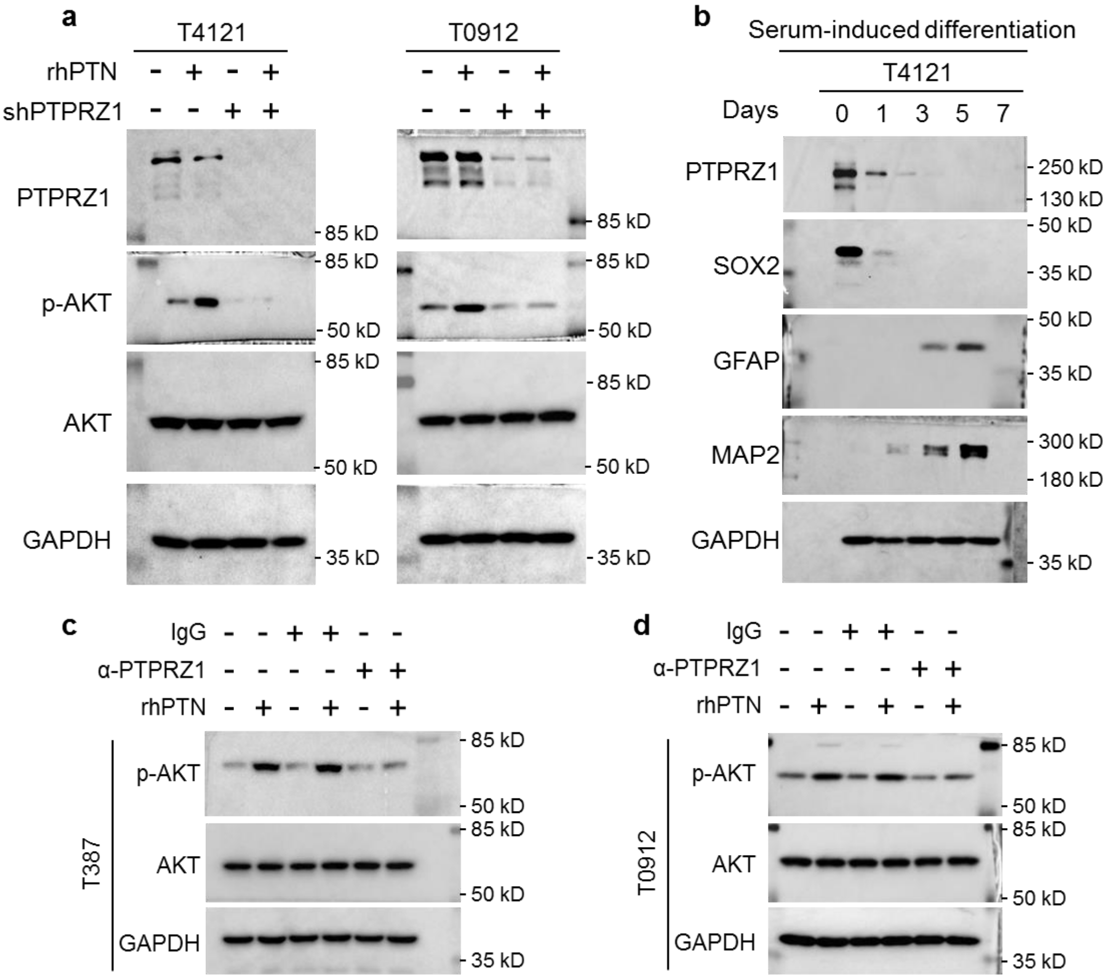

Supplementary Figure 12. Original scans of representative full-length blots in the main figures.

(**a**) Immunoblot analyses of PTPRZ1, phospho-AKT (p-Ser473) and total AKT in GSCs expressing shPTPRZ1 or shNT in combination with rhPTN stimulation.

(**b**) Immunoblot analyses of PTPRZ1, the GSC marker SOX2, the astrocytic differentiation marker GFAP and the neuronal differentiation marker MAP2 in GSCs cultured in serum-induced differentiation medium over a 7-day period.

(**c-d**) Immunoblot analyses of phospho-AKT (p-Ser473) and total AKT in T387 GSCs (**c**) and T0912 GSCs (**d**) upon rhPTN and/or anti-PTPRZ1 antibody treatment.

Supplementary Table 1 Quantifications of SOX2, PTN or CD163 positive cells of in human GBMs.

Patient ID	% of SOX2$^+$ cells		% of CD163$^+$ cells		% of PTN$^+$ cells	
	Average	Standard Deviation	Average	Standard Deviation	Average	Standard Deviation
GBM0358	19.20%	7.33%	11.40%	3.97%	15.60%	5.03%
GBM0867	42.80%	11.01%	10.20%	3.83%	21.00%	7.00%
GBM1305	33.20%	12.03%	10.00%	2.92%	22.00%	5.66%
GBM1435	56.60%	13.65%	22.20%	6.30%	41.20%	11.10%
GBM1866	44.40%	15.53%	9.20%	3.70%	13.20%	3.56%
GBM4668	59.80%	12.91%	11.20%	2.77%	27.00%	7.00%
GBM4981	68.00%	16.08%	27.60%	5.94%	38.60%	8.20%
GBM5450	27.80%	9.86%	10.40%	3.44%	15.20%	5.07%
GBM2399	67.40%	14.84%	24.20%	7.36%	26.20%	6.65%
GBM6702	45.80%	8.17%	9.20%	2.49%	17.80%	4.82%
GBM7010	59.80%	14.84%	11.40%	5.03%	19.40%	5.03%
GBM7511	34.40%	13.13%	16.00%	6.32%	16.00%	3.87%
GBM7857	68.00%	14.02%	19.60%	6.58%	25.80%	6.98%
GBM8847	62.20%	12.87%	34.40%	11.59%	33.20%	8.73%
GBM9146	30.40%	10.48%	10.00%	3.54%	15.40%	4.67%
GBM0156	73.40%	15.44%	22.60%	6.43%	31.20%	8.67%
GBM4730	12.80%	4.97%	3.60%	1.95%	4.20%	2.59%
GBM3126	58.80%	14.65%	11.20%	4.09%	14.20%	5.07%
GBM6079	15.20%	6.18%	1.00%	0.71%	2.60%	2.07%
GBM7503	69.80%	13.41%	24.80%	6.98%	32.80%	7.26%

Abbreviations: GBM, Glioblastoma.

Supplementary Table 2 The overlapped upregulated genes in GSCs relative to NSTCs from both GDS3885 and GSE54791 gene expression profiles.

Gene	GSCs/NSTCs (GDS3885)	GSCs/NSTCs (MGG8)	GSCs/NSTCs (MGG6)	GSCs/NSTCs (MGG4)
PTPRZ1	**284.2**	**106.6139**	**624.8375**	**132.7656**
FABP7	147.74	10.08799	34.77892	194.9979
GPM6B	118.175	30.8512	81.20673	62.398
FXYD6	83.62	25.1358	15.1378	21.46844
S100B	77.78	170.6224	265.7078	205.7967
OLIG1	58.98	357.0636	282.235	115.3386
PMP2	39.25	159.9883	251.1959	49.80343
SOX8	34.7	42.76171	139.8296	112.4571
MLC1	33.49	108.3228	20.27441	10.52407
OLIG2	30.22	162.8567	254.4103	143.4052
MAP2	29.795	35.55822	97.47352	17.4938
SOX2	29.32333	51.12857	44.66943	37.82426
NCAN	25.98	83.68638	283.8979	579.0954
LHFPL3	24.34	67.79991	27.8575	3.173257
INSM1	21.76	12.17771	283.7458	3.984551
AIF1L	18.94	44.08958	109.0063	25.56094
RNF157	18.51	81.00799	23.52447	16.44765
ABAT	18.085	9.232167	13.80151	3.371962
SLAIN1	17.83	13.69892	7.09865	75.33327
C1orf61	17.82667	126.8359	283.226	15.18785
SCRG1	17.61	109.0686	135.7286	14.57756
LOC100506421	17.27	19.24312	105.978	12.66922
GNG7	17.07	12.47806	14.7929	15.6755
SLC35F1	16.47	42.01335	38.04914	25.47074
PTN	16.3	3.218268	4.174727	17.20702
TTYH1	13.98	109.5139	232.4419	83.70676
HES6	13.87	8.323347	12.75646	28.96647
GPRC5B	13.32	10.61411	8.487462	46.80197
KIF5C	11.86	4.294404	4.780516	8.037809
LPHN3	11.4175	82.02413	7.043419	36.52589
ASCL1	11.35333	268.0327	147.1108	135.3764
CPVL	11.27	40.15137	8.964373	19.64955
CHD7	10.905	6.792906	16.52242	42.43733
CKB	10.82	18.0026	5.516465	3.483312
COL9A3	10.66	113.2781	189.9681	37.42095
PEG3	9.555	9.558056	47.7629	5.20987
GAS7	9.462	34.11968	137.8827	61.28899
BMP7	9.405	125.0853	40.72697	182.4509
CERS1	9.07	19.80103	21.08558	9.636814
PREX1	8.71	6.960822	11.89368	5.536499
LSAMP	8.605	21.52411	4.926939	14.56914
KCNQ2	8.13	302.386	20.62636	44.32335
NPAS3	8.07	6.296905	5.1753	3.883754
MAP3K1	7.6	7.754265	12.98774	4.105784

TUBB2B	6.745	9.161784	10.72267	15.99255
C8orf46	6.695	39.45976	32.31601	6.751572
PPP1R14C	6.37	14.07802	5.721182	229.8719
TMEM198	6.35	19.33576	3.399607	5.234361
ELOVL2	6.1	42.85471	27.38499	4.831071
ETV4	6.07	4.958348	13.6188	3.966295
ATP1B2	6.05	21.21876	209.9979	37.80505
NLGN4X	5.98	43.24325	3.317387	24.92908
TNFRSF19	5.79	50.53871	5.157408	6.115593
B3GAT1	5.62	5.356394	49.04268	94.54959
FOS	5.51	236.4087	8.959965	7.295587
NOTCH1	5.33	10.20499	7.901075	4.301373
FGFBP3	5.08	73.51515	19.95837	26.4541
KIF21A	5.055	5.89221	19.3974	10.84724
CYFIP2	4.93	4.4851	3.384014	4.87878
MANEAL	4.64	14.36268	3.370203	4.645122
GNG4	4.573333	30.19385	24.72519	12.94752
LDLRAD3	4.5	3.4707	7.860397	12.45414
CPXM1	4.44	35.40068	430.711	50.68503
RTKN	4.42	3.368384	3.651618	3.41792
METRN	4.04	17.44902	16.00526	4.948844
SBK1	3.95	7.468824	9.872813	47.32056
GOLM1	3.9	4.229261	4.823762	4.579978
DHRS13	3.82	18.06053	10.81561	3.301548
FAM19A5	3.72	35.7709	6.085051	132.8813
CA14	3.69	220.3728	4.102199	12.71834
ISYNA1	3.61	15.65274	7.843448	3.854048
EPHB3	3.59	39.80339	5.250148	6.669024
EYA2	3.51	8.578824	449.6803	135.5749
TRAF4	3.49	6.376761	3.737991	3.578133
DBI	3.46	5.918128	8.199854	3.230083
BMP8B	3.44	77.72659	31.13967	23.74176
NDRG2	3.33	37.44697	41.96949	84.37755
LPPR5	3.25	74.98744	126.3963	36.87843
TMEM121	3.24	4.180507	4.795929	4.653788
SCG3	3.09	49.7505	33.70296	157.5403
NAT8L	3.07	57.58645	52.47291	116.3892
KCNF1	3.05	7.20778	6.873389	18.44829
CTXN1	3.02	3.959728	4.972054	5.23158

Abbreviations: GSCs, glioblastoma stem cells; NSTCs, non-stem tumor cells. MGG4, 6 and 8, primary GBM cell lines from dataset GSE54791.

Supplementary Table 3 Pathological characteristics of human GBMs used in this study.

Specimen	Histopathology	WHO Grade	Gender	Age	Predominant side of tumor location	Predominant lobe of tumor location	Extent of surgical resection
GBM4730	GBM	IV	Male	77	Left	Frontal	GTR
GBM5385	GBM	IV	Male	64	Right	Occipital	GTR
GBM4303	GBM	IV	Male	61	Left	Frontal	GTR
GBM4157	GBM	IV	Male	50	Left	Frontal	GTR
GBM3126	GBM	IV	Male	62	Right	Parietal	GTR
GBM2833	GBM	IV	Female	25	Left	Frontal	GTR
GBM2399	GBM	IV	Male	44	Right	Temporal	PR
GBM7503	GBM	IV	Male	67	Left	Parietal	GTR
GBM4668	GBM	IV	Female	51	Right	Parietal	GTR
GBM0358	GBM	IV	Male	53	Both	Frontal	PR
GBM0867	GBM	IV	Male	61	Right	Frontal	PR
GBM1218	GBM	IV	Male	50	Left	Temporal	PR
GBM1305	GBM	IV	Male	40	Right	Temporal	GTR
GBM1435	GBM	IV	Male	58	Right	Temporal	GTR
GBM1866	GBM	IV	Male	64	Right	Temporal	PR
GBM4798	GBM	IV	Female	33	Left	Temporal	GTR
GBM4981	GBM	IV	Female	64	Right	Parietal	GTR
GBM5450	GBM	IV	Male	61	Left	Frontal	GTR
GBM6702	GBM	IV	Male	71	Right	Temporal	GTR
GBM7010	GBM	IV	Male	58	Right	Temporal	PR
GBM7511	GBM	IV	Female	58	Left	Temporal	PR
GBM7857	GBM	IV	Male	51	Right	Frontal	GTR
GBM8847	GBM	IV	Male	47	Right	Frontal	GTR
GBM9146	GBM	IV	Female	25	Left	Occipital	PR
GBM9387	GBM	IV	Male	53	Right	Parietal	GTR
GBM0156	GBM	IV	Male	77	Right	Temporal	GTR
GBM6079	GBM	IV	Male	48	Left	Frontal	GTR
GBM3446	GBM	IV	Male	75	Left	Temporal	PR
GBM9360	GBM	IV	Female	64	Left	Parietal	GTR

Abbreviations: GBM, Glioblastoma; GTR, Gross total resection; PR, Partial resection.

Supplementary Table 4 Short hairpin RNA sequences used for lentiviral vector construction.

Vector	Sequence (5' to 3')
shNT (for PTN)	CCGGCAACAAGATGAAGAGCACCAACTCGAGTTGGTGCTCTTCATCTTGTTGTTTTT
shPTN-1	CCGGTCAGCAAACAGGATCAGTTAACTCGAGTTAACTGATCCTGTTTGCTGATTTTTG
shPTN-2	CCGGAGGCAAGAAACAGGAGAAGATCTCGAGATCTTCTCCTGTTTCTTGCCTTTTTT
shNT (for PTPRZ1)	TTCTCCGAACGTGTCACGT
shPTPRZ1-1	GCACAAGAATCGATACATA
shPTPRZ1-2	CGAAGGAACTGTCAACATA

Supplementary Table 5 Primers used for qRT-PCR analyses in this study.

Gene	Forward primer (5' to 3')	Reverse primer (5' to 3')
CD163	TTTGTCAACTTGAGTCCCTTCAC	TCCCGCTACACTTGTTTTCAC
PTN	GGAGCTGAGTGCAAGCAAAC	CTCGCTTCAGACTTCCAGTTC
ADM	ATGAAGCTGGTTTCCGTCG	GACATCCGCAGTTCCCTCTT
CDL14A1	TTCAGACTGGTTCGGCATTTC	CTGTGCAAGACCAATTCGTGT
GDF3	TCCTGGAGATACTGGTCAAAGAA	GAGCATCTTAGTCTGGCACAG
IGFBP3	AGAGCACAGATACCCAGAACT	GGTGATTCAGTGTGTCTTCCATT
SPARCL1	CCAACTGAAGGTACATTGGACAT	CTGTGAAGGAACTAACACCAGG
DNER	AAGGCTATGAAGGTCCCAACT	CTGAGAGCGAGGCAGGATTT
IGFBP2	GACAATGGCGATGACCACTCA	CAGCTCCTTCATACCCGACTT
MMP10	TCAGTCTCTCTACGGACCTCC	CAGTGGGATCTTCGCCAAAAATA
TFPI2	TCCTGCCCCTAGACTACGG	CTCCCAGGTGTAGAAATTGTTGG
Fizz1	AGAGTACAGTCCCTCTCC	AACCACAGCCATAGCCACAA
Arg1	TGGACAGACTAGGAATTGGCA	CCAGTCCGTCAACATCAAAACT
CD206	CGATCCGACCCTTCCTTGAC	TGTCTCCGCTTCATGCCATT
iNOS	TTCAGTATCACAACCTCAGCAAG	TGGACCTGCAAGTTAAAATCCC
MHCII	GAGCAGGTTAAACATGAGTGTCA	CTCTCCACAACCCCGTAGT
PTPRZ1	GCCTGGATTGGGCTAATGGAT	CAGTGCTCCTGTATAGGACCA
SOX2	TACAGCATGTCCTACTCGCAG	GAGGAAGAGGTAACCACAGGG
ADD2	ACACCTATGTCACGTTGAGAGT	TCTCCCAGAATGTTCACCTTGA
FYN	TGGAGGTGTGAACTCTTCGTC	TCTGTCCGTGCTTCATAGTCA
CTNNB1	AGCTTCCAGACACGCTATCAT	CGGTACAACGAGCTGTTTCTAC
GIT1	AGCCTTGACTTATCCGAATTGG	CACCTCGTCATACACGTCCA
SLC7A1	GCCTGTGCTATGGCGAGTTT	ACGCTTGAAGTACCGATGATGTA
ALK	TCTCATCGCAGCCGATATGG	GGCATCTCCTTAGAACGCTCT
ARHGAP35	GACTTTTCAACCTCATCGAAGCA	GCTTTCCGTCTGGCATTTGTT
ACTB	CTCCTCCGAGTCAACAGATTCA	CAACAGCTTCTGAGGTAGGGA
GAPDH	AAGGTGAAGGTCGGAGTCAAC	GGGGTCATTGATGGCAACAATA